

Polystyrene nanoparticles facilitate the internalization of impermeable biomolecules in non-tumour and tumour cells from colon epithelium

Laura Cabeza · Victoria Cano-Cortés ·
María J. Rodríguez · Celia Vélez · Consolación Melguizo ·
Rosario M. Sánchez-Martín · Jose Prados

Received: 19 January 2014 / Accepted: 12 December 2014 / Published online: 15 January 2015
© Springer Science+Business Media Dordrecht 2015

Abstract Advanced colon cancer has a poor prognosis due to the limited effectiveness of current chemotherapies. Treatment failures may be avoided by the utilization of nanoparticles, which can enhance the effects of antitumor drugs, reduce their side effects and increase their directionality. Polystyrene nanoparticles have shown high biocompatibility and appropriate physicochemical properties and may represent a novel and more effective approach against colon cancer. In the present study, polystyrene nanoparticles were synthesized and fluorescently labelled, analyzing their cell internalization, intracellular localization and capacity to release transported molecules

in tumour and non-tumour human colon cell lines (T84 and CCD-18). Flow cytometry and fluorescence microscopy studies demonstrated that polystyrene nanoparticles are an effective vehicle for the intracellular delivery of small molecules into colon epithelium cells. The percentage cell uptake was around 100 % in both T84 and CCD-18 cell lines after only 24 h of exposure and was cell confluence-independent. The polystyrene nanoparticles showed no cytotoxicity in either colon cell line. It was found that small molecules can be efficiently delivered into colon cells by using a disulphide bridge as release strategy. Analysis of the influence of the functionalization of the polystyrene nanoparticles surface on the internalization efficiency revealed some morphological changes in these cells. These results demonstrate that polystyrene nanoparticles may improve the transport of biomolecules into colon cells which could have a potential application in chemotherapeutic treatment against colon cancer.

Laura Cabeza, Victoria Cano-Cortés, María J. Rodríguez contributed equally to this work.

L. Cabeza · C. Vélez · C. Melguizo (✉) · J. Prados
Department of Human Anatomy and Embryology,
Institute of Biopathology and Regenerative Medicine
(IBIMER), University of Granada, 18100 Granada, Spain
e-mail: melguizo@ugr.es

V. Cano-Cortés · M. J. Rodríguez ·
R. M. Sánchez-Martín (✉)
Department of Pharmaceutical and Organic Chemistry,
University of Granada, 18071 Granada, Spain
e-mail: rmsanchez@ugr.es

V. Cano-Cortés · M. J. Rodríguez ·
R. M. Sánchez-Martín
GENYO, Centre for Genomics and Oncological Research:
Pfizer/University of Granada /Andalusian Regional
Government, 18016 Granada, Spain

Keywords Polystyrene nanoparticles · Colon cancer · Culture cells · Drug release · Disulphide bond

Introduction

The effectiveness of cytotoxic treatment in colon cancer, the third most frequently diagnosed cancer worldwide (Haggar and Boushey 2009; Siegel et al. 2013),

is currently very limited. Despite recent advances in chemotherapy, advanced or recurrent colorectal cancer remains incurable by conventional treatments (Berrino et al. 2007; Prados et al. 2013). Metastases are developed by 25 % of colorectal cancer patients, with a 5-year survival of only 10 % in patients with metastasis at the time of the diagnosis (Labianca and Merelli 2010). The lack of tumour drug specificity, high systemic drug toxicity and development of multidrug-resistance have been implicated in colon cancer treatment failure (Patwardhan et al. 2010). Thus, novel therapeutic strategies are required for patients with the disease in an advanced stage.

Nanotechnology offers the possibility of improving the cytotoxic treatment of cancer by reducing degradation of the drug, improving its transport to the tumour cell cytosol, avoiding drug resistance mechanisms and increasing its specificity (Brigger et al. 2002). In the case of polystyrene nanoparticles (PS-NPs), a wide size range can be synthesized (32 nm–15 μ m) for different biological applications (Oberdöster 1988; Sánchez-Martín et al. 2005; Pellach and Margel 2014). The biocompatibility of polystyrene NPs is dependent on their surface chemistry. The possibility to easily modify the NP surface (Yu and Fei 2013; Sánchez-Martín et al. 2006) represented some advantage over other NP delivery systems since it may improve their biocompatibility, cytotoxicity and in vivo half-life. In addition, the transported molecule can remain attached to the NPs avoiding its passive diffusion in the cytosol. PS-NPs can also be readily conjugated to a broad range of biomolecules, including drugs, peptides, proteins, RNA and DNA (Tsakiridis et al. 2009; Yusop et al. 2011). PS-NPs may therefore improve the transport and release of biomolecules into tumour tissues, and their size, coating (Kulkarni and Feng 2013) and surface charge (Ekkapongpisit et al. 2012) can be modified for specific applications.

The aim of this study was to evaluate the usefulness of PS-NPs as a delivery system in colon cells. For this purpose, we analysed the cellular uptake of fluorescently labelled PS-NPs in tumour (T84) and non-tumour (CCD-18) cell lines derived from colon epithelium, assessing the cell internalization efficiency of the PS-NPs and their capacity to release a small molecule within the cell and testing their toxicity in both human cell lines.

Materials and methods

Synthesis and loading of polystyrene nanoparticles

Two hundred and five nanometer (PDI = 0.043) aminomethyl PS-NPs (Fig. 1a) were prepared by dispersion polymerization as previously described (Unciti-Broceta et al. 2012). All reagents were obtained from Sigma-Aldrich. 205 nm NPs were firstly functionalized with a polyethylene glycol (PEG) spacer as follows: PS-NPs (Fig. 1a) were washed and suspended in dimethylformamide (DMF) (1 ml). Separately, Fmoc-4, 7, 10-trioxa-1, 13-tridecanediamine succinamic acid (Fmoc-PEG-OH) (75 equiv.) was dissolved in DMF (1 ml) with Oxyma and *N,N'*-diisopropylcarbodiimide (DIC) (75 equiv.) and mixed for 10 min. After this time, the solution was added to NPs and mixed for 2 h at 60 °C. Subsequently, the NPs were washed by centrifugation (13,400 rpm; 3–10 min) with DMF, methanol and water to obtain Fmoc-PEGylated NPs (Fig. 1b). Fmoc deprotection was achieved by treatment with 20 % piperidine/DMF (3 \times 20 min) and sequentially wash steps as previously to give PEGylated NPs (Fig. 1c).

Fluorescein isothiocyanate (FITC)-labelled NPs (NP-FITC) (Fig. 1d) were prepared by the addition of 5, 6-carboxyfluorescein (75 equiv.), Oxyma and DIC (75 equiv.) in DMF to PEGylated NPs and mixed at 60 °C for 2 h. Nanoparticles were then sequentially washed as described above. Capping step was carried out by the addition of acetic anhydride (50 equiv.) and *N,N*-diisopropylethylamine (DIPEA) (50 equiv.) in DMF to PEGylated NPs and mixed at 25 °C for 18 h. Nanoparticles were then sequentially washed as described above to achieve acetylated NPs (Fig. 1e). Disulphide NPs (NP-SS-COOH) (Fig. 1f) were prepared by the addition of dithiodipropionic acid (75 equiv.), DIC (37.5 equiv.) in DMF to PEGylated NPs (Fig. 1c) and mixed at 60 °C for 2 h. Nanoparticles were then sequentially washed as described. Conjugation of 4-aminofluorescein to dithiodipropionic acid functionalised microspheres (Fig. 1f) was achieved by mixing for 4 h at room temperature following preactivation of NPs with a 0.1 M solution of 1-ethyl-3-(3-dimethylaminopropyl) carbodiimide (EDC) in 2-(*N*-morpholino) ethanesulphonic acid (MES) (0.1 ml) to yield FITC-labelled disulphide NPs (NP-SS-FITC) (Fig. 1g) (Alexander et al. 2009).

To prepare dual-labelled NPs with Cyanine 5 (Cy5) and FITC (Fig. 2d), PEGylated NP (Fig. 1c) were treated with Fmoc-Lysine(Dde)-OH (75 equiv.), Oxyma (75equiv.) and DIC (75equiv.) in DMF for 2 h at 60 °C. Nanoparticles were subsequently washed as previously described and Fmoc-deprotected with 20 % piperidine/DMF, yielding free amino residues, which were PEGylated as described above to give NPs (Fig. 2a). Subsequently, Dde deprotection was afforded by treatment of NPs with hydroxylamine HCl (0.4 mmol) and imidazole (0.3 mmol) in *N*-methyl-2-

pyrrolidone (NMP) (1 ml) for 1 h. Nanoparticles were subsequently labelled with Cy5 (1 equiv.) in the presence of DIPEA (2.37 equiv.) in DMF and mixed for 18 h at 25 °C yielding Cy-5 labelled NPs (Fig. 2b). After washing, NPs were Fmoc-deprotected and then coupled with dithiodipropionic acid yielding Cy5-labelled NPs (Cy5-NP-SS-COOH) (Fig. 2c). Aminofluorescein conjugation was done as described above to yield bifunctionalized Cy-5-labelled-NP with aminofluorescein conjugated by a disulphide bridge (Cy5-NP-SS-FITC) (Fig. 2d). Particle size

Fig. 1 Strategy for functionalization of nanospheres and cargo conjugation. Reagents and conditions: (i) Fmoc-PEG-OH spacer, Oxyma, DIC, DMF, 2 h, 60 °C, 100 %; (ii) 20 %piperidine/DMF, 3 × 20 min, rt; (iii) 5,6-carboxifluorescein, Oxyma, DIC, DMF, 60 °C, 2 h, 100 %; (iv) acetic anhydride, DIPEA, DMF, 18 h, rt, 100 %; (v) 3-3'-dithiodipropionic acid, DIC, DIPEA, DMF, 2 h, 60 °C, 100 %; (vi) (1) EDC, MES, 25 °C, 4 h, 100 %; (2) 4-amimofluorescein, PBS, 25 °C, 18 h, 100 %

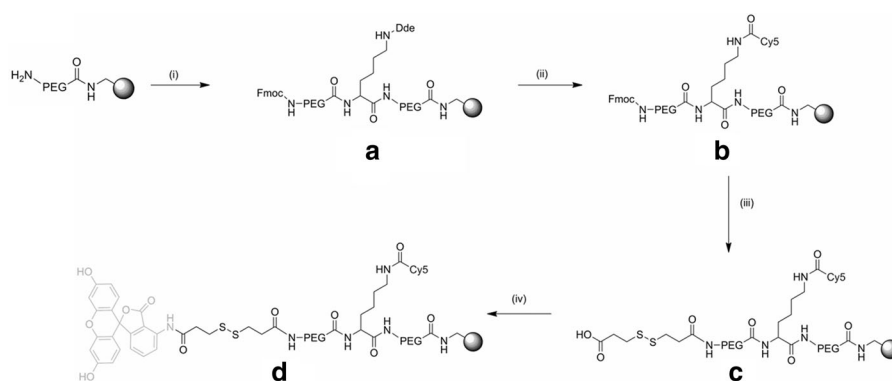
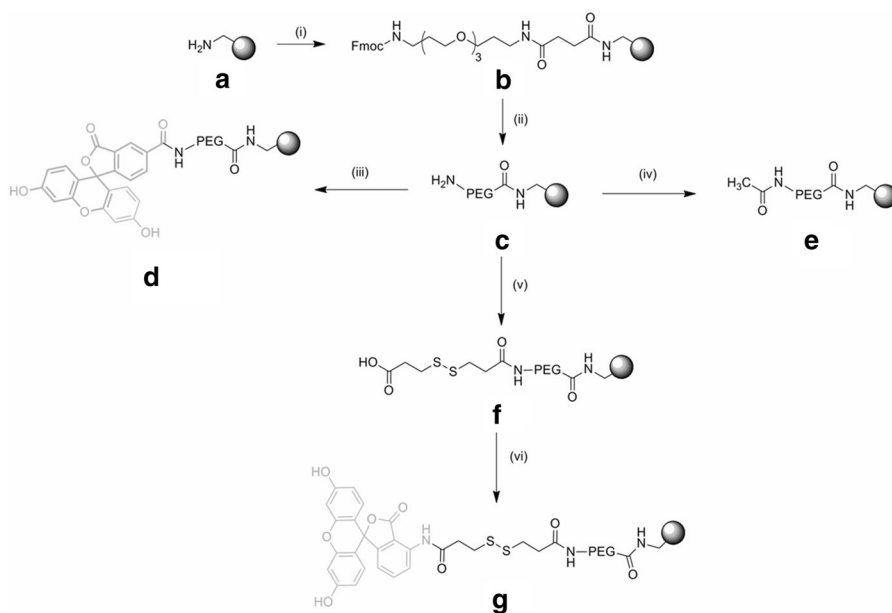


Fig. 2 Strategy for functionalization of dual-labelled nanospheres 200 nm with Cy5 and fluorescein. Reagents and conditions: (i, 1) Fmoc-Lys- Dde(OH), Oxyma, DIC, DMF, 2 h, 60 °C, 100 %; (2) 20 %piperidine/DMF, 3 × 20 min, rt; (3) Fmoc-PEG-OH, Oxyma, DIC, DMF, 2 h, 60 °C, 100 %; (ii,

1) $\text{NH}_2\text{OH}\cdot\text{HCl}$ /imidazole in NMP, 2 × 1 h, rt; (2) Cy5, DIPEA in DMF, 18 h, rt, 100 %; (iii, 1) 20 %piperidine/DMF, 3 × 20 min, rt; (2) 3-3'-Dithiodipropionic acid, DIC, DIPEA, DMF, 2 h, 60 °C, 100 %; (iv, 1) EDC, MES, 25 °C, 1,400 rpm, 4 h, 100 %; (2) 4-aminofluorescein, PBS, 25 °C, 18 h, 100 %

distribution by Dynamic Light Scattering (DLS) and Zeta potential values was measured for each batch of nanoparticles on a Zetasizer Nano ZS ZEN 3500 in molecular biology grade water in a disposable sizing cuvette for size measurements or clear disposable zeta cuvette for zeta potential measurements.

Cell culture

The human colon cancer cell line T84 and the human non-tumour colon cell line CCD-18, obtained from American Type Culture Collection (ATCC, Manassas, VA), were cultured as previously we described (Martín-Banderas et al. 2012).

Flow cytometry assays

T84 and CCD-18 cells were seeded in 6-well plates (15×10^3 cells/well) in 2 ml of complete DMEM. To analyse NPs cell, internalization cells were exposed at 1.08 and 2.16 μM of PEGylated NPs, NP-FITC, and acetylated NPs (Fig. 1c–e) during 24, 48 and 72 h according our previous studies (Tsakiridis et al. 2009; Bradley et al. 2008). Untreated cells and unconjugated fluorescein in solution were used as negative control. In addition, both cell lines were seeded at different cell confluence (10, 25, 50, 65, 80 and 100 %) and exposed to NP-FITC (Fig. 1d) (1.08 and 2.16 μM) during 24 h, in order to determine the influence of cell confluence in NP internalization. To analyse the efficiency of intracellular release using the disulphide bridge as strategy cleavage, both cell lines were exposed for 24 h at a concentration of 1.08 μM of unlabelled disulphide NPs (Fig. 1f), Cy5-labelled disulphide NPs (Fig. 2c) and the same NPs conjugated to aminofluorescein, NP-SS-FITC (Fig. 1g) and Cy5-NP-SS-FITC (Fig. 2d), respectively. Fluorescence intensity of FITC ($\lambda_{\text{emission}} = 520$ nm) and Cy5 ($\lambda_{\text{emission}} = 670$ nm) was measured with a flow cytometer BD FACSCanto II.

Fluorescence microscopy

T84 and CCD-18 cells were seeded (2×10^3 cells/well) in chamber slides (BD Biosciences, Erembodegem, Belgium) with 300 μl of complete DMEM and exposed at 1.08 and 2.16 μM of unlabelled PEGylated NPs (Fig. 1c) and NP-FITC (Fig. 1d) for 24, 48 and 72 h. Then, cells were washed with PBS, fixed with

methanol 10 min at -20 °C and mounted using Ultra Cruz™ Mounting Medium (Santa Cruz Biotechnology, Heidelberg Germany). Samples were evaluated using a Nikon Eclipse 50i microscope (Nikon Instruments Inc., Melville, NY).

Cytotoxicity studies

T84 and CCD-18 cells were seeded in 24-well plates (8×10^3 cells/well) in 400 μl of complete DMEM. Culture cells were exposed at six concentrations (0.27–8.64 μM) of PEGylated NPs (Fig. 1c) for 24, 48 and 72 h. Sulphorhodamine B assay was carried out to evaluate the cellular cytotoxicity of NPs as previously we described (Martín-Banderas et al. 2012).

Statistic analysis

The results were analysed with the Student's *t* test ($\alpha = 0.05$) using the Statistical Package for the Social Sciences v.15.0 (SPSS). All data shown were represented as mean \pm standard deviation (SD).

Results and discussion

Synthesis and loading of polystyrene nanoparticles

A monodispersed population of 205 nm aminofunctionalized cross-linked PS-NPs (PDI 0.043) (Fig. 1a) was obtained by dispersion polymerization as previously described (Unciti-Broceta et al. 2012). PEGylation of PS-NPs (Fig. 1b) was performed following a Fmoc solid phase protocol and using Oxyma/DIC as coupling reagents. This PEGylation increases the biocompatibility of the NPs, thereby facilitating their transport across cell membranes. It also reduces unfavourable interactions between NPs and the bioactive cargoes. Surface functionalization was performed by reacting PEGylated NPs (Fig. 1c) with acetic anhydride in order to coat them with acetyl groups (Fig. 1e). The NPs were conjugated to 5, 6-carboxyfluorescein to allow quantification of their uptake with a fluorescence-based technique (Fig. 1d). An intracellular cleavable linker, dithiopropionic acid, was conjugated to PEGylated NPs as a release strategy (Fig. 1f); this disulphide bridge is cleaved by intracellular glutathione, releasing the desired cargo. Aminofluorescein, used as a model drug, was

conjugated to the NPs using a water-soluble carbodiimide (Fig. 1f). The uptake efficiency of the cleavable NPs was assessed by double-functionalizing them using orthogonally protected lysine (Fmoc-Lysine(Dde)-OH) (Díaz-Mochón et al. 2004). Hence, the NPs were conjugated simultaneously to a fluorophore (Cy5) and to the desired cargo, i.e. aminofluorescein (Fig. 2d). The size homogeneity of resulting nanoparticles was checked routinely by DLS. Efficiency of conjugation was routinely monitored by measurement of zeta potential values for each sample. As previously described, the zeta potential values of modified nanoparticles correlated to the nature of chemical modification (Thielbeer et al. 2011). The zeta potential of the initial amino-functionalized nanoparticle was $+25 \pm 3$ mV, then zeta potential shifts to $+3$ mV when NP were PEGylated and to -5 mV when they are acetylated, allowing us to monitor each step.

Nanoparticle cell internalization studies

Polystyrene nanoparticles cell internalization studies

Cell internalization of NPs was evaluated in T84 and CCD-18 cell lines by flow cytometry and fluorescence microscopy using NP-FITC (Fig. 1d). Carboxyfluorescein alone, which cannot penetrate through the cell membrane at the concentration used (Kim et al. 2012), was used as control (see “Materials and methods” section). The internalization efficiency of NP-FITC after 24 h of exposure was nearly 100 % in the T84 and CCD18 cells at the highest concentration (2.16 μ M) indicating that all analysed cells internalize NPs. However, CCD18 cells at the lower concentration (1.08 μ M) did not reach the 100 % of the internalization efficiency. In any case, the internalization efficiency of NP-FITC in both T-84 and CCD18 cells was significantly higher than in the case of FITC alone at both concentrations 1.08 and 2.16 μ M ($p < 0.001$). In addition, we observed a little but significant difference in the internalization efficiency of NP-FITC at the concentration of 1.08 μ M between both cell lines ($p = 0.004$) (Fig. 3a). On the other hand, NP-FITC at the lower concentration (1.08 μ M) induced a greater fluorescence intensity in T-84 cells in relation to CCD-18 cells only after 48 h of exposure (Fig. 3b) ($p = 0.042$) suggesting a best internalization of the NPs in tumoral cells at least at this time. In any

case, NPs improve the penetration of the molecule in both tumoral and non-tumoral cells.

These results were corroborated by the fluorescence microscopy findings. T84 and CCD-18 cells exposed to NP-FITC showed an intense fluorescence (Fig. 4a) although with a no homogeneous internalization rate. As expected, cells exposed to free fluorescein did not emit fluorescence, indicating that this molecule was internalized by conjugation to the NPs. These NPs showed an intracellular localization in both cell lines (Fig. 4a). These results are in agreement with data published by Sánchez-Martín et al. (2009) using the same PS-NPs in human cervix carcinoma (HeLa) and melanoma (B16F10) cells. A microscopy analysis by Alexander et al. (2010) detected no presence of membrane around these NPs, suggesting passive entry; however, this mechanism remains unclear.

Influence of surface chemical groups on cellular uptake of Polystyrene nanoparticles (PS-NPs) by colon cells

PEGylated NPs without fluorophores but with amino groups ($-\text{NH}_2$) (Fig. 1c) or acetyl groups ($-\text{COCH}_3$) (Fig. 1e) on their surface were used to analyse the influence of these surface groups on NP internalization. Flow cytometry showed a markedly greater incorporation of amino-functionalized versus acetylated nanoparticles in both T84 and CD-18 cells (Fig. 4b). Interestingly, amino groups induced a significant change in the inner complexity of T84 cells that was not observed using acetylated NPs (Fig. 4c). A lesser change was observed in CCD-18 cells (Fig. 4b). These results may explain the difference in cellular uptake between the cell lines (see above). Some authors have hypothesized that a positive charge on the NP surface can increase the cellular uptake in comparison to a neutral or negative charge (Kenzaoui et al. 2012; Alexis et al. 2008).

Release efficiency of aminofluorescein

Utilization of a disulphide bridge has been reported to achieve the efficient intracellular release of conjugated bioactive molecules from different types of NP (Zhao et al. 2011; Borger et al. 2011) within beadfected cells by glutathione activity (Wu et al. 2004). T84 and CCD-18 cells exposed NP-SS-FITC (Fig. 1g) showed

Fig. 3 Polystyrene NPs cell internalization. Flow cytometry analysis after cells exposure (24, 48 and 72 h) to NP-FITC (1.08 and 2.16 μ M) and FITC alone which was used as a control. **a** Study of percentage cell uptake. **b** Study of median fluorescence intensity. Both studies showed significant differences between NP-FITC and FITC ($*p < 0.001$) and between 1.08 and 2.16 μ M ($\#p < 0.001$) in both cell lines T-84 and CCD18. Values represent mean \pm SD of four different cultures

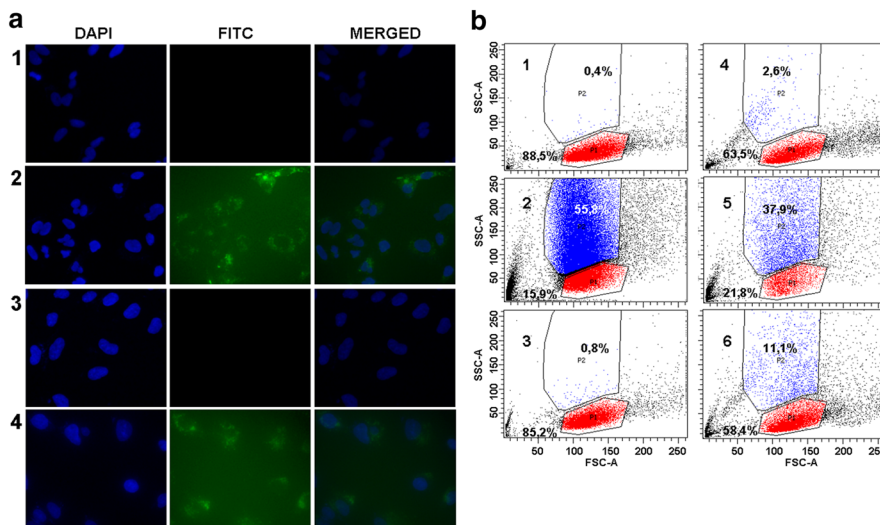
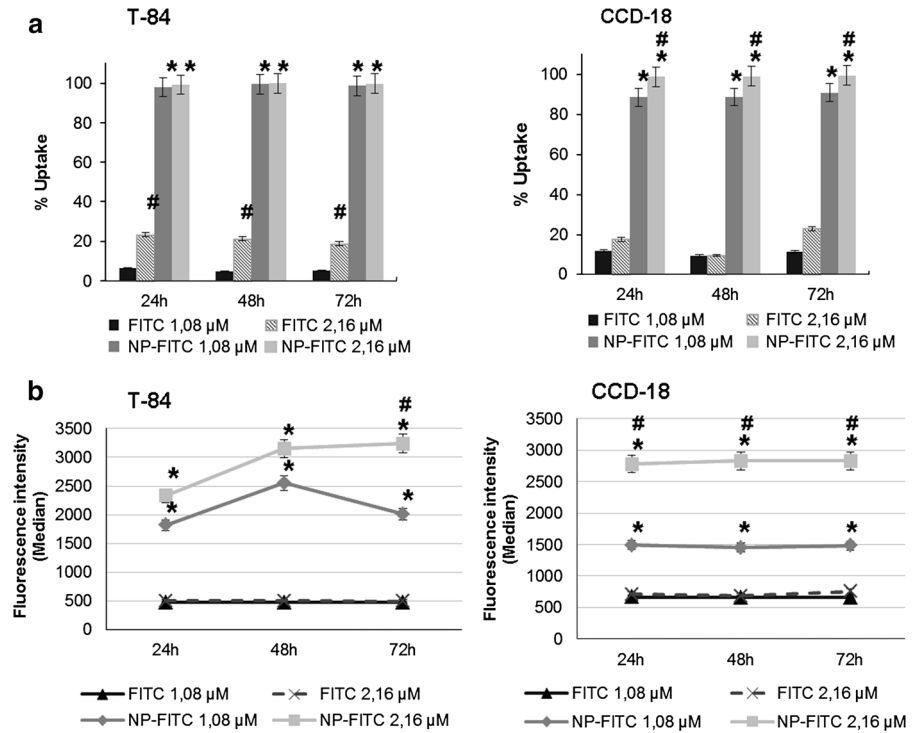


Fig. 4 Polystyrene NPs cell internalization. **a** Fluorescence microscopy analyses using NP-FITC. No fluorescence was observed in either T84 (a1) or CCD-18 (a3) cells treated with the control solution (FITC alone). In contrast, cytoplasmatic fluorescence was observed in both T84 (a2) and CCD-18 (a4) cells after NP-FITC exposure (2.16 μ M after 72 h). All samples were nucleus-stained with DAPI. All images, 20 \times

magnification. **b** Flow cytometry analysis of cell complexity after exposure to NPs modified with surface chemical groups (NH₂ and COCH₃). Untreated T84 and CCD-18 cells (c1 and c4), T84 and CCD-18 cells treated with NP-NH₂ (c2 and c5), and T84 and CCD-18 cells treated with NP-COCH₃ (c3 and c6). All exposures were performed at 1.08 μ M for 24 h

a decrease in fluorescence intensity (in a time-dependent manner) in comparison to the NP-FITC-treated cells (control) (Fig. 5). These findings suggest that aminofluorescein is released in the cytoplasm after cleavage of the disulphide bridge inside the cells and that its leakage can take place within a short period of time (Ormerod 2000).

Bi-functionalized Cy-5-labelled NPs with aminofluorescein conjugated via a disulphide bridge (Cy5-NP-SS-FITC) (Fig. 2d) were evaluated in order to monitor the cell uptake of these NPs and to ensure that the disulphide bridge was cleaved within the cell. As can be observed in Fig. 5c, both T84 and CCD-18 cells showed an intense Cy5 fluorescence but very low FITC fluorescence, demonstrating that aminofluorescein is released from the NPs within the cells and that the NPs remain in the cell cytosol. This result demonstrated that disulphide bridge may be used to insure the molecule release inside colon cells.

Effect of polystyrene nanoparticles on cell proliferation

Because PS-NPs are not biodegradable, no side effects are produced by degradation products, and cytotoxicity has usually been related to the concentration and amino group content of the NPs (Yu and Fei 2013). The size and shape of NPs also play a role, with smaller and spherical NPs evidencing lesser toxicity (Fritz et al. 1997). PS-NPs were previously reported to have no toxic effects on different cell types, including adherent, suspension and primary cells (Ekkapongpisit et al. 2012; Tsakiridis et al. 2009; Alexander et al. 2010). We found no significant differences between T84 and CCD-18 cells treated with PEGylated NPs and the control cells at the different exposure times and concentrations (Fig. 6). Only at the highest PEGylated NP concentration (8.64 μM) and exposure (72 h), CCD-18 showed some growth decrease (35 %) probably by cell overloading.

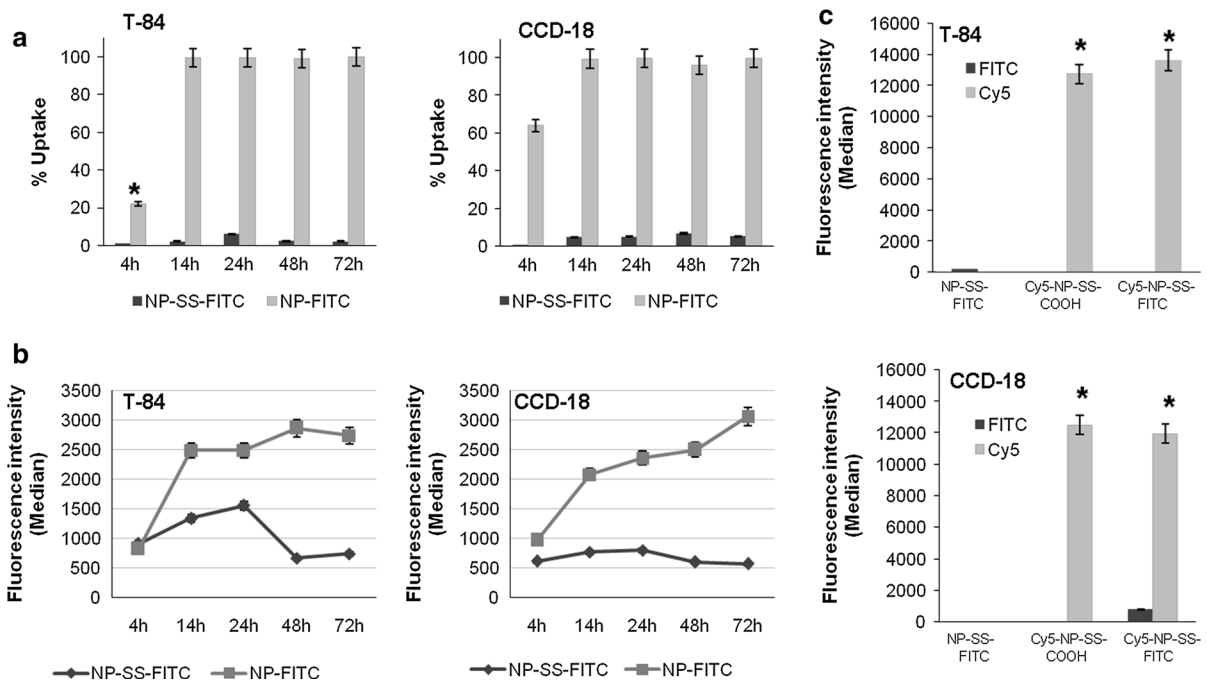
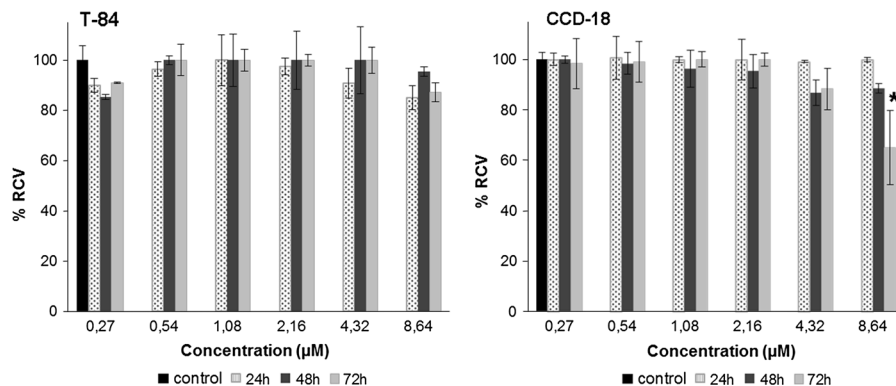


Fig. 5 Release efficiency of polystyrene NPs. Flow cytometry analysis of disulphide bridge breakage showing percentage cell uptake of NP-FITC and NP-SS-FITC (both 2.16 μM) at different exposure times (a) and median FITC fluorescence intensity with the same treatments (b). NP-SS-FITC cellular uptake and fluorescence intensity showed significant differences ($p < 0.05$) compared to NP-FITC. Flow cytometry analysis with

double labelling (c) showing median of the fluorescence intensity of Cy5 and FITC in cells after exposure of NP-SS-FITC and Cy5-NP-SS-FITC. Cy5-NP-SS-COOH was used as a control. All treatments were performed at 1.08 μM for 24 h. Cy5 fluorescence intensity showed significant differences ($*p < 0.05$) compared to FITC. Values represent mean \pm SD of four different cultures

Fig. 6 Proliferation analysis of cell cultures after NP-FITC exposure. Percentage relative cell viability (RCV) of cell lines treated with increasing concentrations of NP-NH₂ at 24, 48 and 72 h of exposure. Untreated cells were used as control. Values represent mean \pm SD of three different cultures



Conclusion

This study examined the usefulness of PS-NPs for transporting anti-tumour drugs in colon cancer treatments. Results obtained demonstrate that these PS-NPs facilitate the internalization of impermeable compounds in both tumour (T84) and non-tumour (CCD-18) colon cells and are not toxic for either cell type. The incorporation of disulphide bridges proved to be an appropriate strategy for releasing an active ingredient within these cells. The present findings suggest that these NPs may be useful as a novel method to achieve the delivery of drugs in colon cancer patients.

Acknowledgments This study was funded by Fondo Europeo de Desarrollo Regional (FEDER) inside of the Plan Nacional de Investigación Científica, Desarrollo e Innovación Tecnológica (I + D + I), Instituto de Salud Carlos III (FIS) through Project no. P111/01862 and by the Consejería de Salud de la Junta de Andalucía through Project no. PI-0049. It was also partially supported by a Marie Curie Career Integration Grant within the 7th European Community Framework Programme (FP7-PEOPLE-2011-CIG-Project Number 294142).

References

- Alexander LM, Sánchez-Martín RM, Bradley M (2009) Knocking (anti)-sense into cells: the microsphere approach to gene silencing. *Bioconjug Chem* 20:4224–42246. doi:[10.1021/bc800529r](https://doi.org/10.1021/bc800529r)
- Alexander LM, Pernagallo S, Livigni A, Sánchez-Martín RM, Brickman JM, Bradley M (2010) Investigation of microsphere-mediated cellular delivery by chemical, microscopic and gene expression analysis. *Mol Biosyst* 6:399–409. doi:[10.1039/b914428e](https://doi.org/10.1039/b914428e)
- Alexis F, Pridgen E, Molnar LK, Farokhzad OC (2008) Factors affecting the clearance and biodistribution of polymeric nanoparticles. *Mol Pharm* 5:505–515. doi:[10.1021/mp800051m](https://doi.org/10.1021/mp800051m)
- Berrino F, De Angelis R, Sant M, Rosso S, Bielska-Lasota M, Coebergh JW, Santaquilani M, EUROCARE Working group (2007) Survival for eight major cancers and all cancers combined for European adults diagnosed in 1995–1999: results of the EUROCARE-4 study. *Lancet Oncol* 8:773–783
- Borger JG, Cardenas-Maestre JM, Zamoyska R, Sanchez-Martin RM (2011) Novel strategy for microsphere-mediated DNA transfection. *Bioconjug Chem* 22:1904–1908. doi:[10.1021/bc200289n](https://doi.org/10.1021/bc200289n)
- Bradley M, Alexander L, Sanchez-Martin RM (2008) Cellular uptake of fluorescent labelled biotin-streptavidin microspheres. *J Fluoresc* 18:733–739
- Brigger I, Dubernet C, Couvreur P (2002) Nanoparticles in cancer therapy and diagnosis. *Adv Drug Deliv Rev* 54:631–651
- Díaz-Mochón JJ, Bialy L, Bradley M (2004) Full orthogonality between Dde and Fmoc: the direct synthesis of PNA-peptide conjugates. *Org Lett* 6:1127–1129
- Ekkapongpisit M, Giovia A, Follo C, Caputo G, Isidoro C (2012) Biocompatibility, endocytosis, and intracellular trafficking of mesoporous silica and polystyrene nanoparticles in ovarian cancer cells: effects of size and surface charge groups. *Int J Nanomed* 7:4147–4158. doi:[10.2147/IJN.S33803](https://doi.org/10.2147/IJN.S33803)
- Fritz H, Maier M, Bayer E (1997) Cationic polystyrene nanoparticles: preparation and characterization of a model drug carrier system for antisense oligonucleotides. *J Colloid Interface Sci* 195:272–288
- Hagar FA, Boushey RP (2009) Colorectal cancer epidemiology: incidence, mortality, survival, and risk factors. *Clin Colon Rectal Surg* 22:191–197. doi:[10.1055/s-0029-1242458](https://doi.org/10.1055/s-0029-1242458)
- Kenzaoui BH, Vilà MR, Miquel JM, Cengelli F, Juillerat-Jeanneret L (2012) Evaluation of uptake and transport of cationic and anionic ultrasmall iron oxide nanoparticles by human colon cells. *Int J Nanomed* 7:1275–1286. doi:[10.2147/IJN.S26865](https://doi.org/10.2147/IJN.S26865)
- Kim K, Kim JA, Lee SG, Lee WG (2012) Seeing the electroperative uptake of cell-membrane impermeable fluorescent molecules and nanoparticles. *Nanoscale* 4:5051–5058. doi:[10.1039/c2nr30578j](https://doi.org/10.1039/c2nr30578j)

- Kulkarni SA, Feng SS (2013) Effects of particle size and surface modification on cellular uptake and biodistribution of polymeric nanoparticles for drug delivery. *Pharm Res* 30:2512–2522. doi:[10.1007/s11095-012-0958-3](https://doi.org/10.1007/s11095-012-0958-3)
- Labianca R, Merelli B (2010) Screening and diagnosis for colorectal cancer: present and future. *Tumori* 96:889–901
- Martín-Banderas L, Alvarez-Fuentes J, Durán-Lobato M, Prados J, Melguizo C, Fernández-Arévalo M, Holgado MÁ (2012) Cannabinoid derivative-loaded PLGA nanocarriers for oral administration: formulation, characterization, and cytotoxicity studies. *Int J Nanomed* 7:5793–5806. doi:[10.2147/IJN.S34633](https://doi.org/10.2147/IJN.S34633)
- Oberdöster G (1988) Lung clearance of inhaled insoluble and soluble particles. *J Aerosol Med* 1:289–330. doi:[10.1089/jam.1988.1.289](https://doi.org/10.1089/jam.1988.1.289)
- Ormerod MG (2000) *Flow cytometry a practical approach*, 3rd edn. Oxford University Press, Oxford
- Patwardhan G, Gupta V, Huang J, Gu X, Liu YY (2010) Direct assessment of P-glycoprotein efflux to determine tumor response to chemotherapy. *Biochem Pharmacol* 80:72–79. doi:[10.1016/j.bcp.2010.03.010](https://doi.org/10.1016/j.bcp.2010.03.010)
- Pellach M, Margel S (2014) Preparation and characterisation of uniform near IR polystyrene nanoparticles. *Photochem Photobiol*. doi:[10.1111/php.12244](https://doi.org/10.1111/php.12244)
- Prados J, Melguizo C, Ortiz R, Perazzoli G, Cabeza L, Alvarez PJ, Rodriguez-Serrano F, Aranea A (2013) Colon cancer therapy: recent developments in nanomedicine to improve the efficacy of conventional chemotherapeutic drugs. *Anticancer Agents Med Chem* 13:1204–1216
- Sanchez-Martin RM, Muzerelle M, Chitkul N, How SE, Mittoo S, Bradley M (2005) Bead-based cellular analysis, sorting and multiplexing. *ChemBioChem* 6:1341–1345
- Sánchez-Martín RM, Cuttle M, Mittoo S, Bradley M (2006) Microsphere-based real-time calcium sensing. *Angew Chem Int Ed Engl* 45:5472–5474
- Sanchez-Martin RM, Alexander L, Muzerelle M, Cardenas-Maestre JM, Tsakiridis A, Brickman JM, Bradley M (2009) Microsphere-mediated protein delivery into cells. *ChemBioChem* 10:1453–1456. doi:[10.1002/cbic.200900136](https://doi.org/10.1002/cbic.200900136)
- Siegel R, Naishadham D, Jemal A (2013) Cancer statistics, 2013. *CA Cancer J Clin* 63:11–30. doi:[10.3322/caac.21166](https://doi.org/10.3322/caac.21166)
- Thielbeer F, Chankeshwara SV, Bradley M (2011) Polymerizable fluorescein derivatives: synthesis of fluorescent particles and their cellular uptake. *Biomacromolecules* 12:4386–4391
- Tsakiridis A, Alexander LM, Gennet N, Sanchez-Martin RM, Livigni A, Li M, Bradley M, Brickman JM (2009) Microsphere-based tracing and molecular delivery in embryonic stem cells. *Biomaterials* 30:5853–5861. doi:[10.1016/j.biomaterials.2009.06.024](https://doi.org/10.1016/j.biomaterials.2009.06.024)
- Unciti-Broceta A, Johansson EM, Yusop RM, Sánchez-Martín RM, Bradley M (2012) Synthesis of polystyrene microspheres and functionalization with Pd(0) nanoparticles to perform bioorthogonal organometallic chemistry in living cells. *Nat Protoc* 7:1207–1218. doi:[10.1038/nprot.2012.052](https://doi.org/10.1038/nprot.2012.052)
- Wu G, Fang YZ, Yang S, Lupton JR, Turner ND (2004) Glutathione metabolism and its implications for health. *J Nutr* 134:489–492
- Yu L, Fei X (2013) Synthesis, characterization and biological evaluation of functionalized polystyrene particles. *J Nanosci Nanotechnol* 13:5814–5822
- Yusop RM, Unciti-Broceta A, Johansson EM, Sánchez-Martín RM, Bradley M (2011) Palladium-mediated intracellular chemistry. *Nat Chem* 3:239–243. doi:[10.1038/nchem.981](https://doi.org/10.1038/nchem.981)
- Zhao M, Biswas A, Hu B, Joo KI, Wang P, Gu Z, Tang Y (2011) Redox-responsive nanocapsules for intracellular protein delivery. *Biomaterials* 32:5223–5230. doi:[10.1016/j.biomaterials.2011.03.060](https://doi.org/10.1016/j.biomaterials.2011.03.060)